KARGER

Cells Tissues Organs in vivo, in vitro

Supplementary Material

Original Paper

Embryonic Stem Cells Facilitate the Isolation of Persistent Clonal Cardiovascular Progenitor Cell Lines and Leukemia Inhibitor Factor Maintains Their Self-Renewal and Myocardial Differentiation Potential in vitro

Julia Hoebaus, Philipp Heher, Teresa Gottschamel, Matthias Scheinast, Harmen Auner, Diana Walder, Marc Wiedner, Jasmin Taubenschmid, Maximilian Miksch, Thomas Sauer, Martina Schultheis, Alexey Kuzmenkin, Christian Seiser, Juergen Hescheler, Georg Weitzer

Cells Tissues Organs 2013;197:249-268 (DOI: 10.1159/000345804)

Suppl Material (61356KB)

Online Supplementary Material

Hoebaus, J., et al. (2013) Embryonic stem cells facilitate the isolation of persistent clonal cardiovascular progenitor cell lines and leukemia inhibitor factor maintains their self-renewal and myocardial differentiation potential in vitro. Cells Tissues Organs, DOI: 10.1159/000345804

On the Probability to Generate CVPCs by Reprogramming, Transdifferentiation, or Cell-Cell Fusion Followed by Reductive Mitosis during the Isolation Procedure of Endogenous CVPCs from Mouse Hearts

The isolation procedure for putative CVPCs was based on several experimentally determined border conditions and conclusions by analogy, drawn from ESC biology, and can be best described by the mathematical model presented in fig. S1A. We started with 500.000 somatic heart cells (SHCs) from mice of different age, mixed them with 500.000 embryonic stem cells (ESCs), and plated them on 150.000 mitotically inactivated SNL76/6 fibroblasts on a 2 cm^2 plate on day 0 of the isolation procedure (table S1). To specifically select for putative self-renewing cells present in the heart we chose a modified 3T3 protocol as expansion regime. Mixed cells were grown at high density for 3 days. On the third day confluence of the ESCs was reached. Then the cells were split 1:3 and 1/3 of the cells, irrespective of their number, was plated on a new feeder cell plate. This procedure was repeated ten times. The chosen number of ESCs together with the splitting regime guaranteed a nearly constant presence of ESCs over all 10 passages of the modified 3T3 protocol (fig. S1A). We chose to repeat expansion and splitting only ten times and not 20 to 30 times used in the original 3T3 protocol to minimise the change to obtain artificial cells by cell fusion, transdifferentiation, or reprogramming. From pilot experiments we knew that primary SHCs (i) divide rarely one or

two times in culture but mostly not at all, (ii) constantly die during in vitro culture with a daily rate of 10 ± 5%, and (iii) decrease in number when transferred to a new culture dish by 50 ± 20%, due to their inability to survive trypsinization and their inability to re-attach properly to the culture plate and SNL76/7 feeder cells. We further assumed the presence of at least one CVPC with a latent self-renewal potential in the population of the 500.000 SHCs, based on assumptions published by Piero Anversa and colleagues [Beltrami et al., 2003]. The doubling time of these CVPCs was expected to be shorter than 36 hours. Consequently, under the regime of splitting cells 1:3 every third day, CVPCs would increase in number, while the number of ESCs would roughly stay constant, and post-mitotic SHCs would rapidly decrease in number (fig. S1A). Splitting 1:3 instead of plating a defined and fixed number of cells every third day promotes fast growing cells and thus allows enrichment of self-renewing CVPCs.

Table S1. Border conditions and experimentally determined parameters on which the modified 3T3 protocol is based

Cell type	Fraction of dying cells		τ[1] (h)	N(P0)	N(P10)
	daily	during splitting			
SHC	0.1	0.5	>78	500.000	0
CVPC	<0.01	0.3	26	≥1	314[2]
ESC	<0.01	0.3	34	500.000	2.500.000[3]

[1] Estimated mean doubling time in dense to confluent culture plates. SHC, were supposed to be post-mitotic (τ>78hours), thus in a 78 hour (3 day) 1:3 splitting regime, SHC, would constantly decrease in number. In the mathematical model presented in fig.S1A, τ was increased by 40% on the third day of each passage for ESCs and CVPCs (only after passage 4) to take reduced proliferation during confluence into account.

[2] Number of colonies counted after the first round of selection with G418 for heart-derived self-renewing cell colonies.

[3] Experimentally determined maximal possible number of ESCs in a 2 cm^2 plate after 3 days.

To demonstrate the isolation procedure graphically we developed a mathematical model with the border conditions as presented in table S1 (fig. S1A). The number of cells n_x for each day during the selection protocol was calculated by

$$n_x = \exp (\ln n_{x-1} + 24 * \ln 2/\tau) - DT * n_{x-1}$$

where DT is the death toll during splitting of cells, x the day, and τ is the doubling time for the cells. Starting from passage one, SHC rapidly decrease in number and are gone by day 20 at the latest. Monitoring the culture plates daily, we were not able to see any heart-derived cell after day 9 because more than 99.9% of the cells in the plate were ESCs. When the isolation procedure was repeated, cells with morphology similar to the CVPCs isolated in the first round appeared as soon as the majority of heart cells had died or were diluted out (fig. S1B).

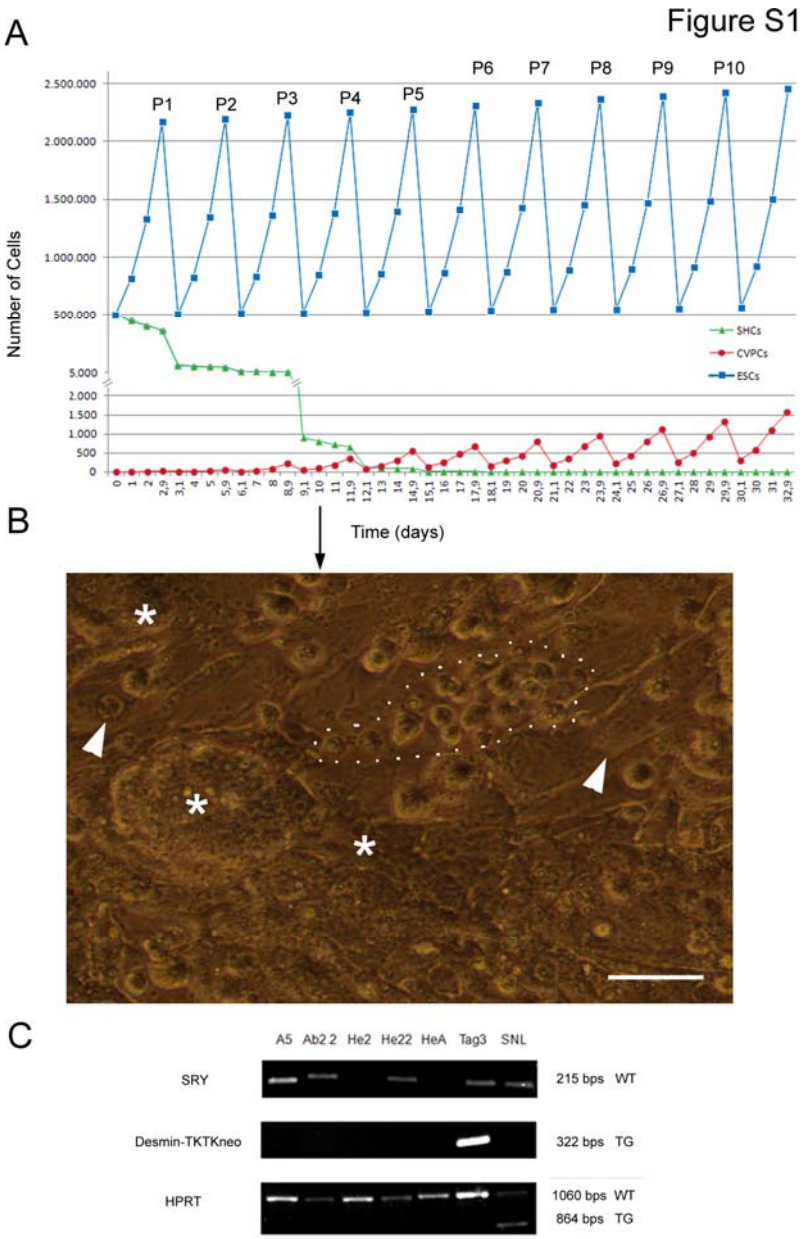

Fig. S1. Isolation of CVPCs from murine hearts. (**A**) Simulation of cell numbers during the isolation procedure of CVPCs. SHC, somatic heart cells; CVPCs, cardiovascular progenitor cells; ESCs, embryonic stem cells; P, passage. For experimentally set boundary conditions see table S1. (**B**) First CVPCs become visible in the presence of SNL76/ feeder cells and ESCs at passage 3 (P3). A clone of very small cells resembling CVPCs is encircled by a dotted line and is clearly distinguishable from ESCs (asterisks) and SNL76/7 fibroblasts (arrowheads) one day after plating of P3 (day 10 of the isolation procedure, see arrow in A). Phase contrast micrograph. Bar: 20 µm. (**C**) PCR with primers specific for the *Hprt* locus on the X chromosome demonstrate that SNL76/7 fibroblasts with an inserted neo transgene (TG) did not fuse with heart cells to give rise the He2, He22, and HeA CVPCs. Likewise, absence of the Desmin-TkTkneo transgene located on chromosome 1 of Tag3 ESCs demonstrates that Tag3 ESCs did not fuse with heart cells to give rise to the He2, He22, and HeA CVPCs. Finally, the absence of the *Sry* gene located on the Y chromosome in He2, and HeA CVPCs demonstrate that these CVPC lines must have been derived from the female mouse and again excludes fusion with the "male" Tag3 ESCs and SNL76/7 fibroblasts.

This mathematical model allows to estimate the chances that reprogramming, transdifferentiation or cell fusion might be the reason for obtaining self-renewing cells which were not present in the original population of SHCs at the beginning of the modified 3T3 protocol. If reprogramming or transdifferentiation is involved in this isolation procedure it must have happened within 9 days with a probability much greater than 1 in 500.000 because the initially present number of SHCs was set 500.000 and rapidly decreased during the modified 3T3 protocol within 3 days to 61.000 living cells, and further down to 7.400 on day 6 and 900 on day 9. According to the model, the last SHC must have been diluted out on day 21at the latest; practically, after day 10 the remaining SHCs can be neglected. Thus, since all published examples of reprogramming and transdifferentiation took 14 to 21 days before first reprogrammed cells could be identified, and another couple of weeks of culture before they adopted a stable phenotype, and because of the low probability of induced reprogramming of $p < 0.002$ [Ieda et al., 2010], it seems extremely unlikely, if not impossible, to generate reprogrammed or transdifferentiated stable progenitor cells within 21 days from a very small and ever decreasing number of non-dividing SHCs. At this time at the latest (experimental data suggests that this happens already at day 10) all SHCs are dead or diluted out by the splitting regime. However, alteration of the phenotype of the endogenous CVPCs during the isolation procedure cannot be excluded, as this cannot be excluded for any cell type and cell lines isolated from primary cell populations of any origin in the past.

To evaluate the chance of cell-cell fusion we determined the fusion rate of ESCs cultured on SNL76/7 feeder cells by combining 10.000.000 ESC with a Neomycin resistance cassette with 10.000.000 ESCs with a Puromycin resistance cassette, as selectable markers, cultured the mixture for 3 days and selected for fused cells in the presence of Puromycin and G418. Four experiments with a total of 80.000.000 ESCs did not result in a single fused cell colony,

whereas control experiments in the presence of polyethylene glycol resulted in 14 clones of fused, Puromycin and G418 resistant cells with a tetraploid karyotype, out of 10.000.000 ESCs. Thus the probability of spontaneous fusion of ESCs under our culture conditions and within a period of 15 days is less than 1 in 40.000.000 cells which equals a frequency lower than 2.5×10^{-10}. Accounting that the mean of the total number of ESC (5.190.643) and SHCs (152.671) (sum of all cells present for 30 days and 20 day, respectively) is the limiting factor, we immediately see that we would have required more than eight times the number of ESCs and more than 27 times the number of SHCs present during the isolation procedure to obtain a single fused cell. Further, taking into account that (i) fusion of a somatic post-mitotic cell as present in the heart with a stem cell is even rarer than the fusion of highly proliferating cancer cells, which fuse in vitro at a frequency of 10^{-5} to 10^{-7} [Pawelek and Chakraborty, 2008], and (ii) that proliferating bone marrow cells and ESCs fuse spontaneously only at a frequency of 10^{-6} to 10^{-5} per bone marrow cells if IL3 was present, and that no clone was obtained from 4×10^{6} cells in the absence of IL3 [Terada et al., 2002], and (iii) that the mean of the total number of SHC present for 20 days (sum of all cells present for 20 days) was 152.671, the probability to obtain a single SHC-ESC fusion product would have to be larger than 1 in 152.671 ($p= 6.6 \times 10^{-6}$). This value is four orders of magnitude larger than the experimentally determined probability for ESC-ESC fusion (2.5×10^{-10}), consequently we would have needed 10.000 times more cells, present during the CVPC isolation procedure, to obtain a single cell line generated by cell fusion.

Additionally, since cell-cell fusion results in tetraploid cells, one must assume a highly efficient and fast reductive mitosis in those fused cells, to explain the diploid karyotype of the CVPC cell lines (table S2). Reductive mitosis, however, have been demonstrated to be a gradual process taking place in several consecutive cell divisions requiring at least 15 days and happens to a significant extent only in the absence of p53 [Vitale et al., 2010]. Further, it

has been demonstrated that tetraploid cells generated by fusion of bone marrow cells with ESCs do not undergo spontaneous reductive mitosis within at least 49 days [Terada et al., 2002], which makes it very unlikely that this event has occurred once during the 30 day lasting isolation procedure. The facts that even in the absence of p53 not more than 20% of the tetraploid cells became pseudo-diploid [Vitale et al., 2010], that CVPC lines used in this study contained 95% diploid cells, and that they indeed express p53 which prevents reductive mitosis (fig. 2C), strongly suggests that cell fusion in combination with reductive mitosis was not the major mechanism generating the CVPC lines.

Finally, genetic analysis of cell types involved in the isolation procedure and of the isolated clonal CVPC lines (table S3, [Hasties, 1989], figs. 1F, 7B and S1C) strongly suggests that the described CVPC lines indeed originate from the heart tissue, do not contain genetic material from ESCs or SNL76/7 fibroblast, and thus represent the in vitro counterpart of endogenous CVPCs of the heart.

Table S2. Euploidy of CVPCs cells and ESCs

Clone Name	% diploid nuclei	Number of nuclei analysed
A5*	98	160
H3*	95	40
B5*	90	20
G3*	86	43
B3	90	10
C3	60	10
D3	91	11
D5	61	18
A3	67	18
E3	83	35
F3	75	8
He2*	98	50
He22*	96	50
HeA*	90	50
AB2.2	94	119

* These cell lines were used for experiments in this study

Table S3. LINE-1 repetitive DNA element polymorphisms analysis[1, 2]

Restriction Enzyme	EcoRI[3]	Sca I	Hinf I	Sca II + Bsg I
Clone Name	Length of fragments in kbp			
A5	1.4	1.6	1.18	2.2
C3	1.4	1.6	n.d.	2.2
F3	1.4	n.f.d.	n.d.	n.f.d.
AB2.2 (ESCs)	1.3	1.8	1.22+1.48	2.0
SNL76/7 (fibroblasts)	1.3	1.4	1.22+1.48	2.0
C75BL/129Sv (donor mouse)	1.4	n.f.d.	n.d.	2.2

[1][Hasties, 1989]
[2][Rebuzzini et al., 2009]
[3][Bennett et al., 1984]

n.f.d., no fragment detected, n.d., not determined

From these data, border conditions, and constraints discussed above it becomes evident that it is extremely unlikely ($p«10^{-4}$), and practical impossible, to obtain artificial cells with a stable phenotype lasting for 149 passages, from less than 500.000 somatic and mainly post-mitotic cells within less than 20 days by cell-cell fusion and reductive mitosis, reprogramming or transdifferentiation.

Expression of Marker Genes in 11 Clonal CVPC Lines

To demonstrate similar but not identical expression of marker genes in all 11 clonal cell lines of CVPCs obtained from C57BL/6Jx129Sv mice, we cultured these cell lines in parallel and determined expression of Oct4, Sox2, Nanog, Brachyury, Mesp1, GATA4, Nkx2.5, Isl1, and Mef2C by RT-PCR (fig. S2) with primer pairs as described in table S7. All 11 clones expressed comparable amounts of Oct4, Nanog, Sox2, and GATA4, but early mesodermal and myocardial transcription factors were expressed more differently. All clones also gave rise to CMCs and ETCs, and where tested, gave rise to SMCs (table S4).

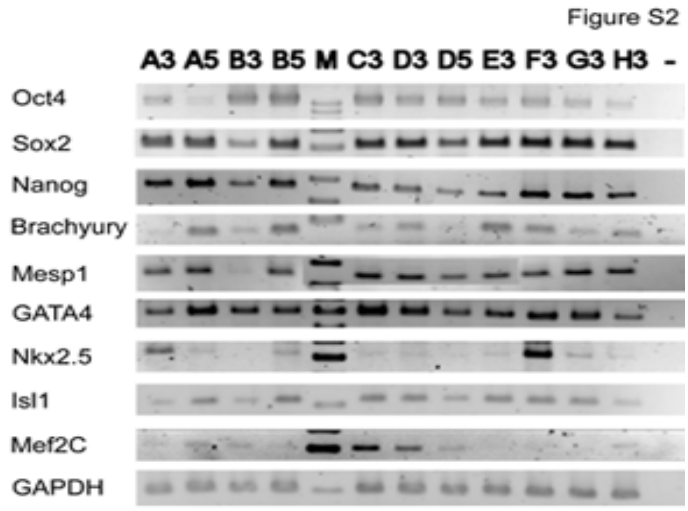

Fig. S2. Gene expression in different clonal CVPC lines. Expression of stemness, early mesodermal, and early myocardial transcription factors in 11 clonal CVPC lines. Semi-quantitative RT-PCR analysis. M, DNA size markers.

Table S4. Contribution of CVPC clones to rhythmically contracting CMCs, slowly contracting SMCs and ETCs in monolayer cultures

Clone Name	Contracting cardiomyocytes	Contracting smooth muscle cells	Endothelial cells
A3	+	n.d.	+++
A5	+++	+++	+++
B3	+	n.d.	+++
B5	++	+++	+++
C3	+	n.d.	+++
D3	++	n.d.	+++
D5	+	+	+++
E3	+	n.d.	+++
F3	++	+	+++
G3	++	++	+++
H3	+++	+	+++
He2	+++	++	+++
He22	++	++	+++
HeA	++	++	+++
Tag3	-	-	-
AB2.2	-	-	-

+++, significant; ++, some; +, few; and -, no parts of the plates were covered with this type of cells; n.d., not determined.

Similar to ESCs, but with a lower frequency, CVPCs displayed an inhomogeneous expression of Oct4 (fig. S3). The percentage of ESCs which have either a significant higher or lower expression of Oct4 was 31.6 +/- 11.3% (N = 101; raw data from [Mateus et al., 2009; Sustackova et al., 2011]), however, in CVPCs we observed fluctuation of Oct4 expression in only 8.8 +/- 8.3% (N = 103) of the cells.

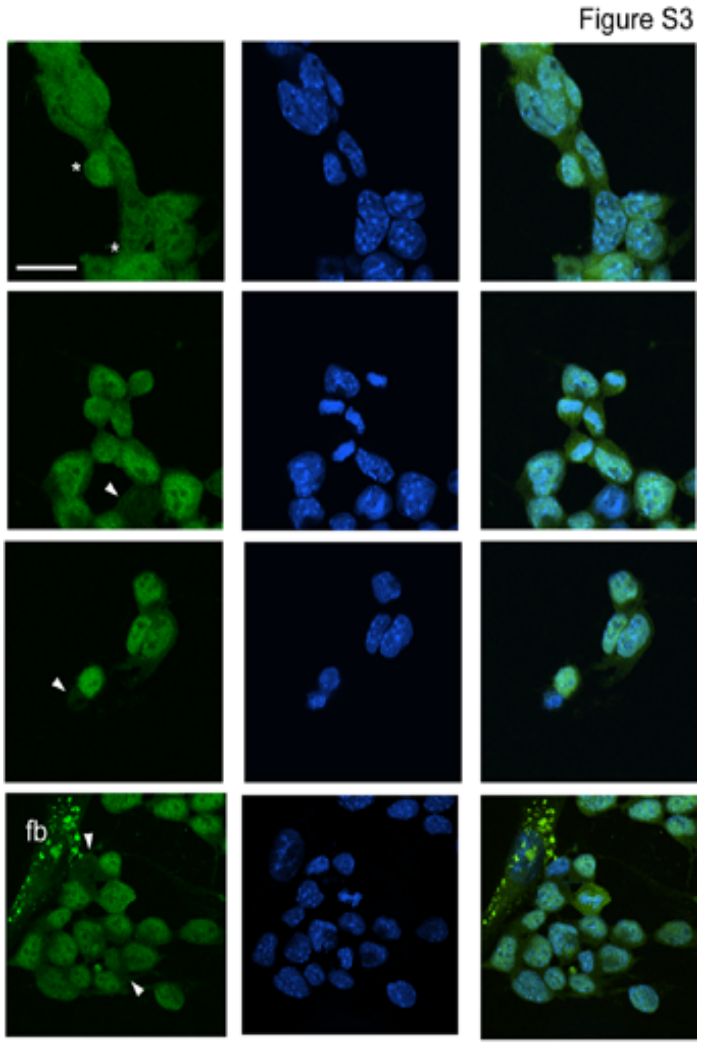

Fig. S3. Fluctuations of Oct4 expression in CVPCs. Immunofluorescence microscopy with anti-Oct4 antibodies (green) and DAPI (blue). Asterisks, CVPCs with higher Oct4 expression; and arrowhead, with lower Oct4 expression. Fb, fibroblast-like cell. Bar: 20μm.

Electrophysiological Characterisation of CVPC-Derived CMCs

We calculated action potential (AP) peak, maximum diastolic potential (MDP), AP amplitude, AP frequency, maximum velocity of depolarization (Vmax), velocity of diastolic depolarization (Vdd), action potential duration at 90% repolarisation (APD90), ratio of APD90/APD50, where APD50 represents action potential duration at 50% repolarisation. AP types: PM, pacemaker-like; A, atrial-like; V, ventricular-like; Ampl, AP amplitude; Freq, AP frequency. Data are presented as the mean ± standard deviation.

Table S5. Action potential parameters for different subtypes of CVPC-derived CMCs at a late developmental stage (day 27)

AP type	Peak (mV)	MDP (mV)	Amp (mV)	Frequency (1/min)	Vmax (V/s)	Vdd (V/s)	APD90 (ms)	APD90/ APD50	N	% of Total
PM	24±9	49±13	70±9	188±89	7±3	0.09±0.04	84±35	1.64±0.28	6	35.3
A	28±19	59±7	87±25	171±46	20±8	0.05±0.02	51±12	2.19±0.43	6	35.3
V	27±3	62±2	90±5	257±66	23±7	0.11±0.05	53±10	1.51±0.08	5	29.4
Total	26±12	56±10	77±26	202±75	16±9	0.08±0.04	63±26	1.51±0.08	17	100

Characterisation of Endothelial Cells in CVPC-Derived CBs

Vessel-like structures formed in areas of CBs with a very high density of epithelia ETCs (fig. S4 A-E). These cells expressed vWF (see fig. 4P), CD31, and Glycogen synthase kinase 3 α/β, both partially located in Weibel-Palade-like bodies (fig. S4 E-G).

Figure S4

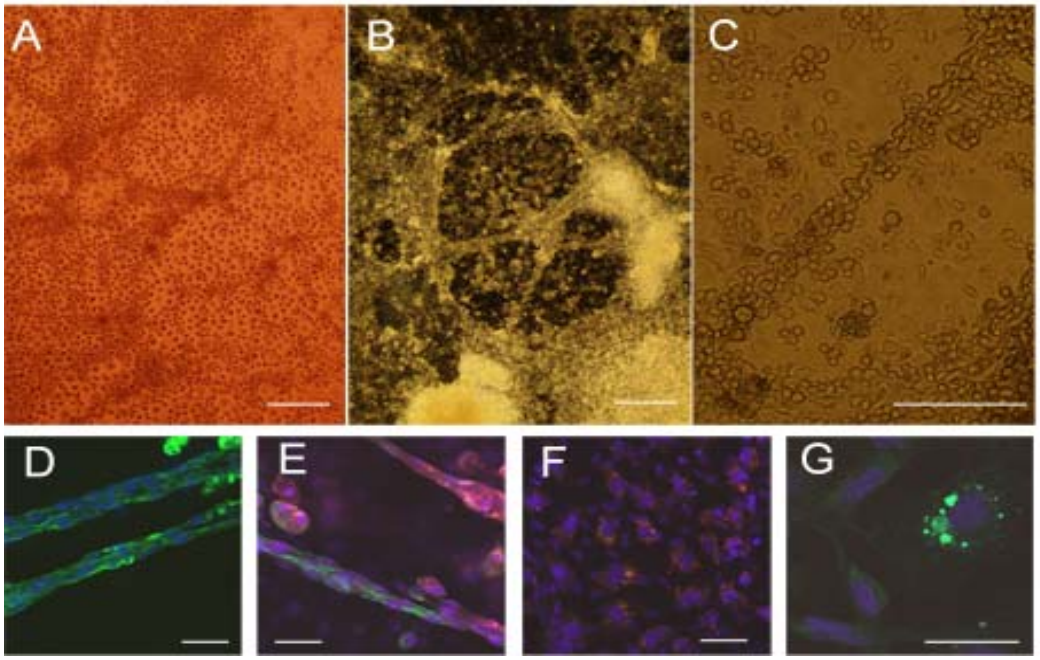

Fig. S4. Characterisation of ETCs in CVPC-derived CBs. (**A**) ETCs at the beginning of vessel-like structure formation at day 17. (**B** and **C**) Vessel-like structures in CBs at day 23. (**D**) Staining of vessel-like structures with anti-SMA antibodies (green), and (**E**) with CD31 antibodies (red). Note, SMA is also present in ETCs [Ando et al., 1999; Azuma et al., 2009]. (**F**) Presence of CD31 and (**G**), Glycogen Synthase Kinase 3 (green) in structures resembling Weibel-Palade bodies in ETCs as previously described [Howell et al., 2004; Niehrs and Acebron, 2010]. Nuclei, DAPI (blue). A-C, phase contrast microscopy. D-G, immunofluorescence microscopy. Bars: A-C, 100μm; D-G, 200μm.

The Inability of CVPCs to Give Rise to Ectodermal and Definitive Endodermal Cells

We aggregated and differentiated CVPCs and ESCs in the presence of Retinoic acid to induce neuro-ectodermal lineage differentiation. Whereas ESC-derived EBs had numerous β3 Tubulin positive cells none of the 60 CVPC-derived CBs examined had a single β3 Tubulin positive cell (fig. S5A and B). RT-PCR analysis further demonstrated that Retinoic acid induced Glial fibrillary acidic protein expression in EBs but not in CBs and increased Thyrosin hydroxylase expression in neurospheres, isolated from N2 murine brain with the same procedure used to isolate CVPCs, but not in CVPC-derived CBs (fig. S5C). Likewise, differentiation of CVPCs in the presence of definitive endoderm inducing concentrations of Activin A, did not result in significant expression of FoxA2 in ETCs, whereas in ESC-derived EBs numerous cells expressed FoxA2 (fig. S5D and E). Cells negative for FoxA2, however, were positive for vWF (fig. S5F). In the presence of Activin A, development of proliferating definitive endoderm islands in EBs was significantly increased, whereas in CBs no definitive endoderm could be detected (fig. S5G).

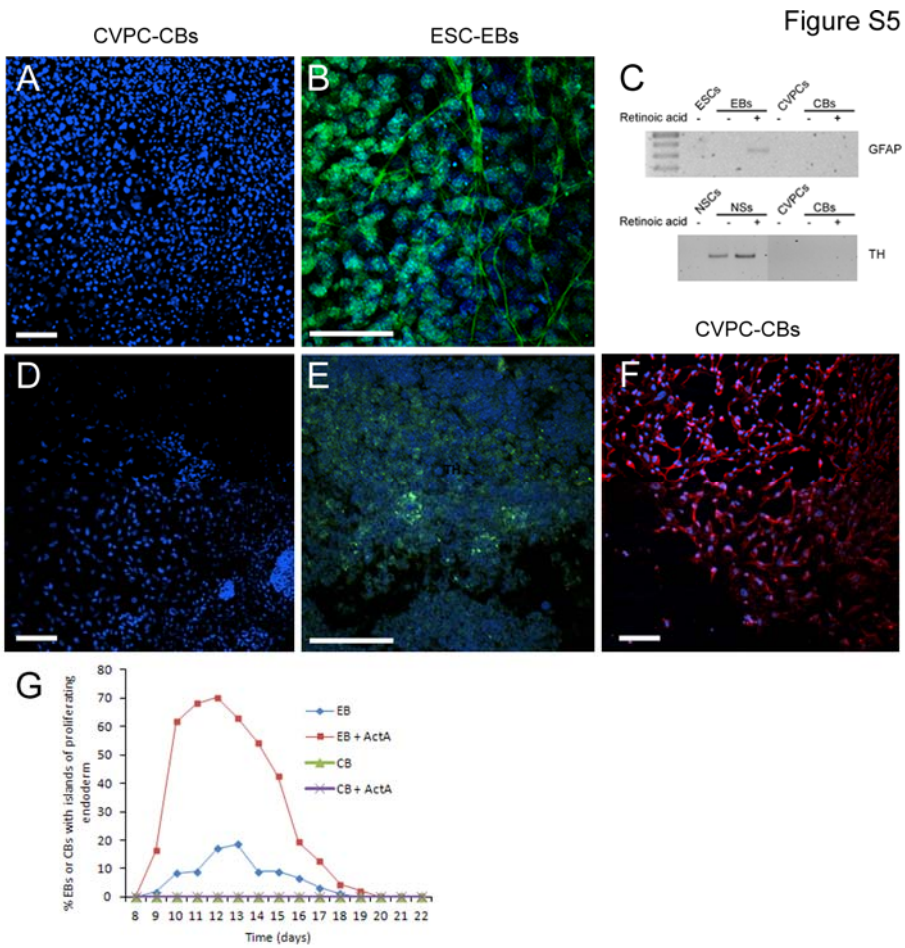

Fig. S5. Absence of any inducing effect of Retinoic acid and Activin A, respectively, in CVPC-derived CBs. (**A** and **B**) Immunofluorescence staining of CBs (**A**) and EBs (**B**) with anti-β3 Tubulin antibodies (green) incubated from day 5 to 20 in the presence of Retinoic acid. (**C**) RT-PCR analysis of undifferentiated (ESCs, CVPCs, and neuronal stem cells (NSCs), respectively) and differentiated cells in the absence and presence of Retinoic acid, in EBs, CBs, and neurospheres (NSs), with primer pairs specific for Glial fibrillary acidic protein und Thyrosin hydroxylase. (**D** and **E**) Immunofluorescence staining of CBs (**D**) and EBs (**E**) incubated from day 5 to 15 in the presence of Activin A with anti-FoxA2 antibodies (green). (**F**) Immunofluorescence staining of CBs with anti-vWF (red). Nuclei, DAPI (blue). Bars: 50 μm. (**G**) Development of proliferating definitive endoderm islands in EBs and CBs. Data are from 2 independent triplicate experiments with one ESC and two CVPC cell lines.

Absence of Skeletal Muscle Myotubes, Neuron-Like Networks, and Erythroblasts in CVPC-Derived CBs

While monitoring CVPC differentiation in more than 1000 CBs during the course of experiments described in this paper we did neither see a single networks of neuron-like cells nor any skeletal muscle fibrils (fig. S6A), whereas in ESC-derived EBs, networks of neuron-like cells (fig. S6B) and skeletal muscle fibrils (fig. S6C), composed of poly-nucleated myotubes (fig. S6D) were frequently observed. In EBs dozens or sometimes hundreds of erythroblasts developed spontaneously in a ring-like structure where primitive mesoderm forms [Fuchs et al., 2012] (fig. S6E), whereas in CBs Benzidine-positive cells were never observed (fig. S6F and G).

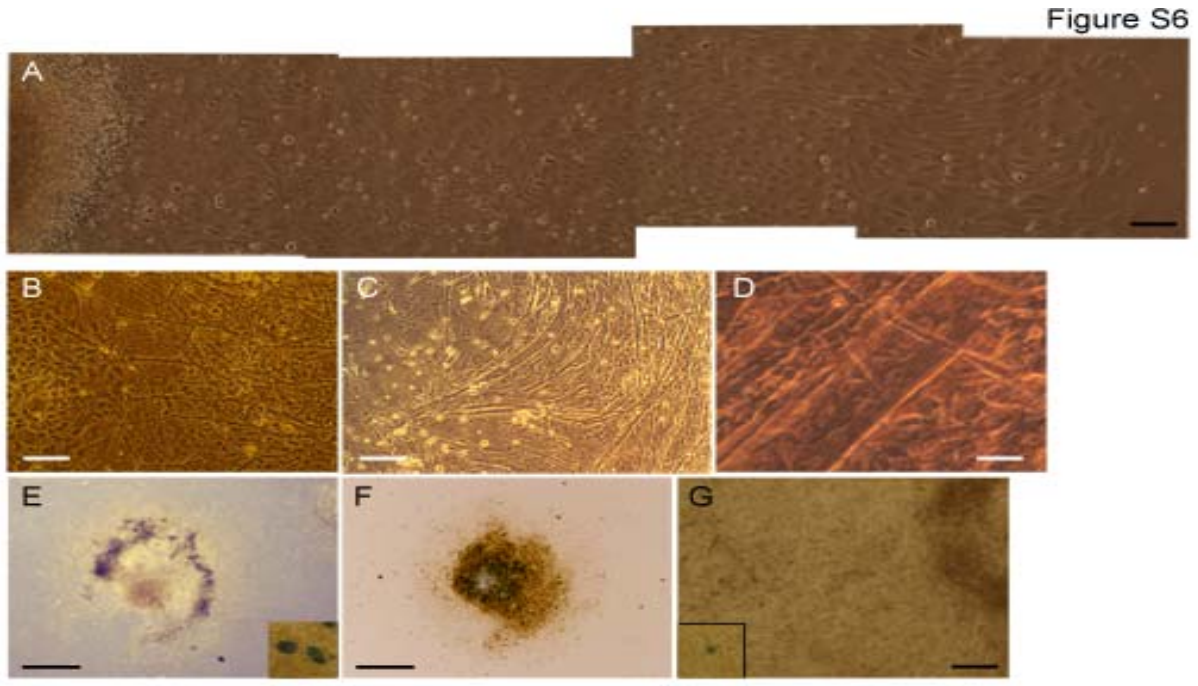

Fig. S6. Absence of skeletal muscle myotubes, neuron-like networks and erythroblasts in CVPC-derive CBs. (**A**) A typical segment of a CVPC-derived CB in which structures as shown in B-D never developed (number of experiments > 100.) The centre of the CB is on the left and the periphery on the right, for orientation please see also figure 4A. In contrast, ESC-derived EBs occasionally developed networks of neuron-like cells (**B**), and frequently contracting skeletal muscle fibres (**C**) and poly-nucleated myotubes (**D**). (**E**) Haemoglobin containing erythroblasts in EBs at day 8 stained with Benzidine (blue cells). Insert, single haemoglobin containing erythroblasts. (**F**) A CBs stained with Benzidine at day 8. Note, dark area is due to the greater density of CBs as compared to EBs, and not a blue stain. (**G**) Area of

a CB stained with Benzidine, where erythroblasts should appear if the were ESC-derived aggregates [Fuchs et al., 2012]. Insert, an image was chosen showing an extremely rare a-cellular blue coloured dust granule, in order to include an internal positive control. A – D, Phase contrast images, and E – G, inclusive inserts, bright field illumination. Bars: A, 50 μm; B and C, 100 μm; D, 10 μm; E and F, 500 μm; G, 100 μm.

Supplementary Methods

Isolation of Heart Cells

Primary CMCs were isolated from E14 129Sv mouse embryos. Heart tissue was digested in the Pancreatin/Collagenase II solution at 37°C for 2 x 15 minutes. CMCs were enriched by adsorption of cardiac fibroblasts at 37°C in M4Si (DMEM supplemented with 4% foetal calf serum (Sigma, #F7425), 2 mmol/l Glutamine, 0.05 mg/ml Streptomycin, and 0.03 mg/ml Penicillin) for 2.5 hours and non-attached CMCs were consecutively cultured in M4Si on gelatine-coated tissue culture plates.

Karyotyping

Confluent cells in a 2 cm^2 plate were fed 1 hour prior to enzymatic dissociation with 200 µl of Trypsin and then transferred to a gelatine-coated 6 well plate in 3 ml of M15Hy medium. After 50 minutes of pre-adsorption half of the cells were transferred onto two gelatine-coated 2 cm^2 plates and incubated at 37°C, 5% CO_2 over night. The following day one of these wells was treated with 10 µl Colchicine (1 mg/ml) for 2 h at 37°C, 5% CO_2. Both wells were trypsinized (200 µl Trypsin) for 15 minutes at 37°C, 5% CO_2 and the reaction was stopped by addition of 800 µl M15Hy. Suspensions were transferred into 15 ml falcon tubes and centrifuged for 5 minutes at 1000 rpm in a Hereaus Megafuge 1.0 centrifuge. Supernatant was disposed and pellets were washed in 1 ml of 1 x PBS twice. The supernatant was removed and 2 ml KCl (37°C, 75mmol/l) were added drop wise under constant swirling. After 7 minutes of

incubation at room temperature the centrifugation step was repeated. Then the supernatant was removed and 4 ml of a methanol : acetic acid (3:1) solution was added and nuclei were incubated at room temperature for 30 minutes. Finally, 1 ml of methanol : acetic acid (1:3) was added to re-suspend the nuclei. Samples were stored at 4°C. Suspended nuclei were dropped onto microscope slides with a Pasteur pipettes. After drops had dried, nuclei were observed with a Zeiss Axiovert 200M microscope and chromosome numbers were counted. Samples were stained with Giemsa stain (Sigma Diagnostics, 1995) diluted 1:20 in ddH_2O and incubated for 15 minutes. Slides were embedded in Mowiol under cover slips.

Measurement of Cell Growth, Size and Number

Doubling time was determined at passage 8 by seeding CVPCs at $1.5x10^5$ cells per well on feeder cells or gelatine-coated 24 well plates. After three days cells were trypsinized, counted, and $1.5x10^5$ cells were transferred onto new gelatine-coated 24 well plates. This process was repeated for 21 days and doubling time was determined for each individual 3 day cycle. The average over all 7 cycles was calculated to obtain the mean doubling time. Cell size was determined by counting pixels of photographs of attached CVPCs and ESCs with Adobe Photoshop 7.0. Cell number and viability was measured with a Casy II counter.

LINE-1 Repetitive DNA Element Polymorphisms Analysis

Genomic DNA was isolated from C57BL/J6-129/SV mice, AB2.2, SNL76/7 cells, and A5 CVPCs and digested with restriction enzymes EcoRI, HinfI, Sca I and Sca II + Bsg I for 3h. DNA fragments were separated on 1.5 agarose gels by electrophoresis and fragmented high copy number LINE-1 DNA elements were detected by ethidiumbromide staining.

Patch-Clamp Analysis

In the current-clamp mode, we recorded action potentials (APs) of the CVPC-derived CMCs. In all experiments, leak subtraction was applied. The extracellular solution contained (in mmol/l): NaCl 140, KCl 5.4, $CaCl_2$ 1.8, $MgCl_2$ 1, Glucose 10, 4-(2-hydroxyethyl)-1-piperazine-ethanesulfonic acid (HEPES) 10, pH adjusted to 7.4 at 37°C with NaOH. Intracellular solution contained (in mmol/l): KCl 50, K-Aspartate 80, $MgCl_2$ 1, MgATP 3, glycol-bis(2-aminoethylether)-N,N,N',N'-tetraacetic acid (EGTA) 10, HEPES 10, pH adjusted to 7.40 with KOH. We have also tested the CMCs for unimpaired hormonal regulation by applying 1 µmol/l Isoproterenol or 1 µmol/l Carbachol.

In the voltage-clamp mode, we recorded voltage-gated Na^+ and L-type Ca^{2+} channel currents. Here the extracellular solution contained (in mmol/l): NaCl 120, KCl 5, $CaCl_2$ 3.6, $MgCl_2$ 1, tetraethylammonium (TEA) chloride 20, HEPES 10, pH adjusted to 7.4 at 37°C with TEA-OH. Intracellular solution contained (in mmol/l): CsCl 120, $MgCl_2$ 3, MgATP 5, EGTA 10, HEPES 5, pH adjusted to 7.40 with CsOH. If not stated otherwise, all substances were purchased from Sigma-Aldrich Chemie GmbH (Germany). Data on L-type Ca^{2+} currents and Na^+ currents were collected simultaneously. Na^+ channel currents were elicited by a family of 100 ms depolarizations from a –90 mV holding potential to voltages ranging from –80 to +40 mV in 5 mV steps. L-type Ca^{2+} channel currents were measured with a double-pulse protocol. First, a 100-ms depolarization from a holding potential of –90 mV to –40 mV was applied to inactivate Na^+ and T-type Ca^{2+} channels, then L-type Ca^{2+} channels were elicited by a family of 100 ms depolarizations with voltages ranging from –60 to +40 mV in 10 mV steps. In Na^+ and Ca^{2+} channel experiments, leak subtraction -P/4 protocol was applied from a holding potential of -90 mV. There was no contamination of L-type Ca^{2+} currents with Na^+, as those were fully inactivated with a long conditioning pre-pulse to –40 mV, before L-

type Ca^{2+} currents were elicited by a test pulse. L-type currents were also always checked for the presence of fast activation component suggesting a contamination with Na^{+} current, and there was no such component visible. The conditioning pre-pulse did not affect L-type Ca^{2+} channels, as they activate in a more positive voltage range. We have also estimated the Ca^{2+} current contamination in Na^{+} currents. As L-type currents were always co-measured in the cells where Na^{+} channel currents were recorded, we compared the amplitudes. If the maxima at corresponding potentials are compared, the mean contamination of Na^{+} currents with an L-type current is less than 1%, whereas in the most relevant voltage range (from –50 to –10 mV) it is less than 0.5%. Considering that the activation of L-type Ca^{2+} channels is 5-10 times slower than the Na^{+} channel activation, we estimated the L-type current contribution to <0.1%. Thus, the Ca^{2+} current contamination in the Na^{+} currents is very small and could be neglected. To estimate the expression of functional ion channels in the cell membrane, we determined current densities by normalizing the maximal current amplitude to the cell size.

Table S6. List of Primers and conditions used for genotyping CVPC lines by PCR

Gene Name		5‘- 3‘ Sequence of oligonucleotides	A.T.	Cycles	Product
Hdac1- Intron 7-Neo transgene	Fwd	TCGCCTTCTTGACGAGTTCTTCT	51°C	50	300 bp
	Rev	TGGCTCACTAAGCTAGGTT			
Hdac1-Exon5	Fwd	GGCCTTGTGTCTTGGAAGAGCAC	58°C	50	317 bp
	Rev	GCTGAAGGAAGGTGGAAGAGTGG			
H60c, C57Bl/6J spec.	Fwd	AGACCTGTGATGAAGATTGCCA	55°C	50	598 bp
	Rev	ACTATGGAACTCAGAGACCCAATC			180 bp
H60b, C57Bl/6J spec.	Fwd	GGCTAGCCATCTGGAACTCAAC	55°C	50	985 bp
	Rev	ACGGGTATACGTCTCTCAAGGA			380 bp
H60a, 129Sv spec.	Fwd	GAAATTGGTGGCGTGCTTGAT	55°C	50	324 bp
	Rev	ACCTGATTGTAACTTCCACATCTCT			500 bp
sPlA2	Fwd	CTGGCTTTCCTTCCTGTCAGCCTGGCC	60°C	50	393 bp
	Rev	GGAAACCACTGGGACACTGAGGTAGTG			
Desmin- Exon 1-TKTKNEO transgene	Fwd	TTCCCTCGAGCAGGCTTCGG	51°C	36	322bp
	Rev	AACAGCGCGGCAGACGTGCG			
Hprt	Fwd	GCTTGCTGGTGAAAAGGACCTC	54°C	36	1062 bp
	Rev	TGGCAACATCAACAGGACTC			364 bp
Sry	Fwd	CCCAGCATGCAAAATACAG	50°C	36	327 bp
	Rev	AACAGGCTGCCAATAAAAGC			

A.T., annealing temperature

Table S7. List of Primers and conditions used for RT-PCR analysis

Gene Name		5‘- 3‘ Sequence of oligonucleotides	A.T.	Cycles	Product
Brachyury	Fwd	GAA CCT CGG ATT CAC ATC GTG AGA	60°C	36	159 bp
	Rev	ATC AAG GAA GGC TTT AGC AAA TGG G			
CD31	Fwd	GTA CTC TAT GCA AGC CTC CA	51°C	33	276 bp
	Rev	CAC TGT GCA TTT GTA CTT CCC G			
CD34	Fwd	GCT GAT GCT GGT GCT AGT	48°C	33	183 bp
	Rev	GCT CCC GAT ATC TTG TTT A			
c-kit	Fwd	GCC CTA ATG TCG GAA CTG AA	49°C	33	319 bp
	Rev	TTG CGG ATC TCC TCT TGT CT			
Desmin	Fwd	TGA CAA CCT GAT AGA CGA	50°C	37	390 bp
	Rev	TTC TTA TTG GCT GCC TGA			
Flk1	Fwd	GCA TGG TCT TCT GTG AGG CAA	51°C	33	620 bp
	Rev	GTT GGT GAG GAT GAC CGT GTA G			
Gata4	Fwd	GCC TGT ATG TAA TGC CTG CG	53°C	31	500 bp
	Rev	CCG AGC AGG AAT TTG AAG AGG			
GAPDH	Fwd	CGT CTT CAC CAC CAT GGA GA	55°C	29	300 bp
	Rev	CGG CCA TCA CGC CAC AGT TT			
GFAP	Fwd	AGG AGC CAG CAG AGG CAG GG	72°C	35	852 bp
	Rev	CTT GGC TTG GCG GAG CAG CT			
Isl1	Fwd	CGG TGC AAG GAC AAG AAA	49°C	38	346 bp
	Rev	CAA TAG GAC TGG CTA CCA			
Mdr1	Fwd	CAT TGG TGT GGT GAG TCA	50°C	34	176 bp
	Rev	CTC TCT CTC CAA CCA GGG TG			
Mef2C	Fwd	GGC CAT GGT ACA CCG AGT ACA ACG AGC	66°C	34	395 bp
	Rev	GGG GAT CCC TGT GTT ACC TGC ACT TGG			
Mesp1	Fwd	AGA AAC AGC ATC CCA GGA AA	52°C	32	346 bp
	Rev	GTG CCT GCT TCA TCT TTA			
Mhcα	Fwd	GGA AGA GTG AGC GGC GCA TCA AGG	57.7°C	32	302 bp
	Rev	CTG CTG GAG AGG TTA TTC CTC G			
Nanog	Fwd	AGG GTC TGC TAC TGA GAT GCT CTG	60°C	25	364 bp
	Rev	CAA CCA CTG GTT TTT CTG CCA CCG			
Nkx2.5	Fwd	CAC CCA CGC CTT TCT CAG TC	57°C	40	513 bp
	Rev	TGG ACG TGA GCT TCA GCA			
Nodal	Fwd	TTC CTT CTC AGG TCA CGT TTG C	58°C	35	519 bp
	Rev	GGT GGG GTT GGT ATC GTT TCA			
Oct3/4	Fwd	CCA CCT TCC CCA TGG CTG GAC A	50°C	37	1082bp
	Rev	AGG GCT GGT GCC TCA GTT TG			
Sox2	Fwd	AAC CCC AAG ATG CAC AAC TC	55°C	34	202 bp
	Rev	CTC CGG GAA GCG TGT ACT TA			
p53	Fwd	CGC TGC TCC GAT GGT GAT GG	64°C	35	343bp
	Rev	TGT CCC GTC CCA GAAGGT TCC			
Tert1	Fwd	AAC CTC CAC CAG CTT ACC CT	58°C	38	398 bp
	Rev	GGG AGC TGT CAC AAG AGG AG			
Tyrosine Hydr.	Fwd	CGT CTC AGA GCA GGA TAC CAA GCA G	71°C	35	835 bp
	Rev	CAG TAG ACC GGC CAC GGG TC			
Tropomyosin α	Fwd	CAA GCG GAG GCT GAT AAG AAG G	55°C	30	310 bp
	Rev	TGC CTC TCT CAC TCT CAT CTG C			

A.T., annealing temperature

Supplementary References

Ando, H., T. Kubin, W. Schaper, J. Schaper (1999) Cardiac microvascular endothelial cells express alpha-smooth muscle actin and show low NOS III activity. Am J Physiol *276*: H1755-H1768.

Azuma, K., K. Ichimura, T. Mita, S. Nakayama, W.L. Jin, T. Hirose, Y. Fujitani, K. Sumiyoshi, K. Shimada, H. Daida, T. Sakai, M. Mitsumata, R. Kawamori, H. Watada (2009) Presence of alpha-smooth muscle actin-positive endothelial cells in the luminal surface of adult aorta. Biochemical and Biophysical Research Communications *380*: 620-626.

Beltrami, A.P., L. Barlucchi, D. Torella, M. Baker, F. Limana, S. Chimenti, H. Kasahara, M. Rota, E. Musso, K. Urbanek, A. Leri, J. Kajstura, B. Nadal-Ginard, P. Anversa (2003) Adult cardiac stem cells are multipotent and support myocardial regeneration. Cell *114*: 763-776.

Bennett, K.L., R.E. Hill, D.F. Pietras, M. Woodworth-Gutai, C. Kane-Haas, J.M. Houston, J.K. Heath, N.D. Hastie (1984) Most highly repeated dispersed DNA families in the mouse genome. Molecular and Cellular Biology 4: 1561-1571.

Fuchs, C., M. Scheinast, W. Pasteiner, S. Lagger, M. Hofner, A. Hoellrigl, M. Schultheis, G. Weitzer (2012) Self-Organization Phenomena in Embryonic Stem Cell-Derived Embryoid Bodies: Axis Formation and Breaking of Symmetry during Cardiomyogenesis. Cells Tissues Organs *195*: 377-391.

Hasties, N.D. (1989) Highly repeated DNA families in the genome of Mus musculus; in Lyon, M.F. and Searls., A. G.(eds): Genetic Variants and Strains of the Laboratory Mouse. Oxford, Oxford University Press, pp 559-573.

Howell, G.J., S.P. Herbert, J.M. Smith, S. Mittar, L.C. Ewan, M. Mohammed, A.R. Hunter, N. Simpson, A.J. Turner, I. Zachary, J.H. Walker, S. Ponnambalam (2004) Endothelial cell confluence regulates Weibel-Palade body formation. Mol Membr Biol *21*: 413-421.

Ieda, M., J.D. Fu, P. Delgado-Olguin, V. Vedantham, Y. Hayashi, B.G. Bruneau, D. Srivastava (2010) Direct reprogramming of fibroblasts into functional cardiomyocytes by defined factors. Cell *142*: 375-386.

Mateus, A.M., N. Gorfinkiel, A.M. Arias (2009) Origin and function of fluctuations in cell behaviour and the emergence of patterns. Semin Cell Dev Biol *20*: 877-884.

Niehrs, C., S.P. Acebron (2010) Wnt signaling: multivesicular bodies hold GSK3 captive. Cell *143*: 1044-1046.

Pawelek, J.M., A.K. Chakraborty (2008) Fusion of tumour cells with bone marrow-derived cells: a unifying explanation for metastasis. Nat Rev Cancer *8*: 377-386.

Rebuzzini, P., R. Castiglia, S.G. Nergadze, G. Mitsainas, P. Munclinger, M. Zuccotti, E. Capanna, C.A. Redi, S. Garagna (2009) Quantitative variation of LINE-1 sequences in five species and three subspecies of the subgenus Mus and in five Robertsonian races of Mus musculus domesticus. Chromosome Res *17:* 65-76.

Sustackova, G., S. Legartova, S. Kozubek, L. Stixova, J. Pachernik, E. Bartova (2011) Differentiation-Independent Fluctuation of Pluripotency-Related Transcription Factors and Other Epigenetic Markers in Embryonic Stem Cell Colonies. Stem Cells Dev *21:* 710-720.

Terada, N., T. Hamazaki, M. Oka, M. Hoki, D.M. Mastalerz, Y. Nakano, E.M. Meyer, L. Morel, B.E. Petersen, E.W. Scott (2002) Bone marrow cells adopt the phenotype of other cells by spontaneous cell fusion. Nature *416*: 542-545.

Vitale, I., L. Senovilla, M. Jemaa, M. Michaud, L. Galluzzi, O. Kepp, L. Nanty, A. Criollo, S. Rello-Varona, G. Manic, D. Metivier, S. Vivet, N. Tajeddine, N. Joza, A. Valent, M.

Castedo, G. Kroemer (2010) Multipolar mitosis of tetraploid cells: inhibition by p53 and dependency on Mos. Embo J *29*: 1272-1284.

Legends for Supplementary Video Files

Supplementary movie 1 Weitzer:	Small cluster of cardiomyocytes at the very beginning of rhythmical contractions in CVPC-derived CBs at day 11
Supplementary movie 2 Weitzer:	Large cluster of mature contracting cardiomyocytes in CVPC-derived CBs
Supplementary movie 3 Weitzer:	Large area of aperiodically and slowly contracting smooth muscle cells in CVPC-derived CBs
Supplementary movie 4 Weitzer:	Increase of smooth muscle cell contraction by Angiotensin II in CVPC-derived CBs at day 24 (Time lapse: x6)
Supplementary movie 5 Weitzer:	Relaxation of Angiotensin II accelerated smooth muscle cell contraction in the presence of Losartan in CVPC-derived CBs (Time lapse: x6)
Supplementary movie 6 Weitzer:	Increase of smooth muscle cell contraction by Angiotensin II in ESC-derived EBs at day 23 (Time lapse: x6) Note, contracting cells in the upper left corner are cardiomyocytes.
Supplementary movie 7 Weitzer:	Relaxation of Angiotensin II accelerated smooth muscle cell contraction in the presence of Losartan in ESC-derived EBs (Time lapse: x6) Note, contracting cells in the upper left corner are cardiomyocytes.